iJRASET
International Journal For Research in Applied Science and Engineering Technology

INTERNATIONAL JOURNAL FOR RESEARCH

IN APPLIED SCIENCE & ENGINEERING TECHNOLOGY

Volume: 14 **Issue:** V **Month of publication:** May 2026

DOI: https://doi.org/10.22214/ijraset.2026.82251

www.ijraset.com

Call: 08813907089 | E-mail ID: ijraset@gmail.com

International Journal for Research in Applied Science & Engineering Technology (IJRASET)
ISSN: 2321-9653; IC Value: 45.98; SJ Impact Factor: 7.538
Volume 14 Issue V May 2026- Available at www.ijraset.com

Enhancing Microgrid Resilience: A Robust Protection Strategy Employing Differential & Overcurrent Relays

Ms. Kalyani Sittalwar[1], Prof. Gaurav Karlekar [2], Prof. V. M. Pimpalkar[3]
[1]*PG Scholar, Department of Engineering, Ballarpur Institute of Technology (BIT), Ballarpur, Maharashtra, India*
[2, 3]*Assistant Professor, Department of Engineering, Ballarpur Institute of Technology (BIT), Ballarpur, Maharashtra, India*

Abstract: ***This research introduces an innovative hybrid adaptive protection system for microgrid systems, enhancing resilience during transitions between grid and islanded modes. Integrating overcurrent and differential relays strategically, the system addresses dynamic variations in short-circuit fault current characteristics. Adaptive overcurrent relays protect distributed generators (DGs) and individual load points (LPs), while differential relays safeguard feeders, backbone lines, and buses, aiming to minimize infrastructure upgrades and simplify setting computations. Through rigorous simulations covering diverse operating conditions, the proposed scheme proves effective in shielding the microgrid from substantial three-phase short-circuit fault currents, enhancing reliability, efficiency, power quality, and stability. Operating adaptively, the scheme uses overcurrent relays for faults outside the protection zone and differential relays for faults within the specified zone, ensuring the safety of consumers and equipment in the microgrid network. Validation through simulations on a typical microgrid test network in MATLAB/Simulink significantly contributes to advancing microgrid system resilience and effectiveness in dynamic operational scenarios.***

Keywords: ***Differential Relay, Microgrid Operation, Grid- Connected Mode, Islanded Mode, Load Points, Reliability Enhancement, Power Quality Assurance, Stability Optimization***

Abbreviations & Nomenclature

LP	Load Points	B1BU	Bus 1 Breaker Unit
SC	Short Circuit	GCM	Grid Connected Mode
CB	Circuit Breaker	RF	Fault Resistance
MG	Microgrid	B	Bus
IM	Islanded Mode	AOCRP	Adaptive Overcurrent Relay Protection
C.T	Current Transformers	MPPT	Maximum Power Point Tracking
R1BU	Radial 1 Breaker Unit	Length of line	L1, L2, L3, L4, L5, L6, and LU = 0.5 km
DSCP	Discriminatory short-circuit protection	ADN	Active distribution networks
DER	Distributed energy resource	DRP	Differential Relay Protection
DG	Distributed Generator	LLL	3 Phase Short circuit faults

I. INTRODUCTION

While research on protection schemes for microgrids is in its early stages, adaptive protection schemes have been proposed, albeit with inherent complexities. Adaptive protection requires advanced technology, self-monitoring capabilities, and complex integration of hardware and software units, demanding significant upgrades to existing infrastructure for practical implementation [1]. Existing protection methods, such as differential schemes utilizing communicative relays, demand extensive communication infrastructure and relay deployment at each line end [2].

In this challenging landscape, this research introduces a hybrid protection scheme, combining differential and adaptive overcurrent relays. The scheme employs differential relays to safeguard microgrid feeders, lines, and interconnecting buses, while adaptive overcurrent relays protect DGs and individual load points.

The integration of DGs into the main grid to form a microgrid offers a viable alternative, leveraging renewable sources for reduced transmission losses, improved power quality, and environmental sustainability [3]. However, challenges arise with the integration of synchronous-based distributed generators (SBDGs) and inverter-based distributed generators (IBDGs) at the sub-transmission or distribution level, particularly concerning overcurrent relay (OCR) protection coordination [4-5]. The operation of microgrids can be categorized into four modes, each presenting unique challenges to traditional protection coordination schemes. Fault currents becoming bi- directional, limitations imposed by inverter-based DGs, and variations in fault current levels due to different generator types contribute to the ineffectiveness of conventional relays [6].

Recognizing the limitations of individual protection methods, the significance of a combined adaptive overcurrent relay and differential relay protection scheme for microgrids becomes evident [7]. Adaptive protection's automatic adjustment to power system conditions and the inherent advantages of differential protection makes this hybrid approach promising for addressing the complexities of microgrid protection [8]. As microgrids continue to evolve, necessitating dynamic protection solutions, this research explores the integration of adaptive and differential protection schemes to enhance the reliability and efficiency of microgrid protection systems. Several studies propose adaptive protection methods for low-voltage microgrids, utilizing communication links for efficient fault detection and relay coordination [9-11]. While these systems provide reliable and fast operation, communication failures remain unaddressed [12]. Alternatives, such as storage-based systems using flywheels, present challenges in on-time fault clearing and require substantial installations [13].

II. CHALLENGES IN EXISTING ADAPTIVE OVERCURRENT RELAY APPROACHES

The current landscape of adaptive overcurrent relay (AOCR) schemes faces critical challenges, particularly in light of evolving distributed energy resource (DER) interconnection requirements and the dynamic transition to microgrid operations. Addressing these challenges is pivotal for advancing the development of versatile AOCR schemes that seamlessly support both grid and microgrid modes of operation.

1) Underreaching OCRs with Multiple DER Generation Levels: Existing AOCR schemes encounter difficulties in accurately estimating fault current contributions from DERs operating at varying output levels. Traditional approaches, treating DERs as constant current sources, may lead to overcompensation or underreaching due to the complex nature of DER behavior [14]. These challenges arise from factors like distance from the fault, fault impedance, and fault type, making it imperative to refine AOCR schemes to account for changing fault current contributions [15].

2) Delayed Trip Time in Microgrid Mode: Microgrids, characterized by lower fault currents compared to grid-connected systems, pose a unique challenge to AOCR sensitivity in primary/secondary protection zones. The traditional time-based coordination methods may introduce significant delays in relay trip times for faults within the primary zone, an aspect often overlooked in existing AOCR approaches [16].

3) Current Direction Reversal during Mode Switching: The possibility of current direction reversal, a phenomenon observed during mode switching in both grid-connected systems and microgrids, remains inadequately addressed in existing AOCR approaches. The lack of attention to directional aspects compromises the selectivity towards internal vs external faults. Incorporating directional supervision is crucial for establishing a robust protection scheme accommodating the coexistence of grid-connected and microgrid modes. Existing AOCR methodologies exhibit limitations in their applicability to active distribution networks (ADNs) embracing both grid and microgrid modes [17]. These approaches are susceptible to under-reaching, struggle with changing fault currents, and may prove overly complex for traditional distribution relays. The subsequent section delves into an emerging vulnerability that challenges conventional practices in relay programming [18].

III. PROTECTION STRATEGIES FOR MICROGRIDS

Differential protection involves assessing the electrical quantities entering and leaving a designated security zone by comparing current through CTs. This method relies on either current balance or voltage balance to determine the absence of faults [19].

Current Balance Differential Protection: This widely utilized principle ensures that under normal conditions, CT currents I_{s1} and I_{s2} are equal ($I_{s1} = I_{s2}$), resulting in no current flow through the relay ($I = I_{s1} - I_{s2} = 0$). In the case of an internal fault at point F within the protection zone, where the fault is fed from both sides, an inverted current through CT_2 triggers the relay ($I = I_{s1} + I_{s2}$). Consequently, the relay activates the Circuit Breaker (CB) associated with the faulty system [13].

ISSN: 2321-9653; IC Value: 45.98; SJ Impact Factor: 7.538
Volume 14 Issue V May 2026- Available at www.ijraset.com

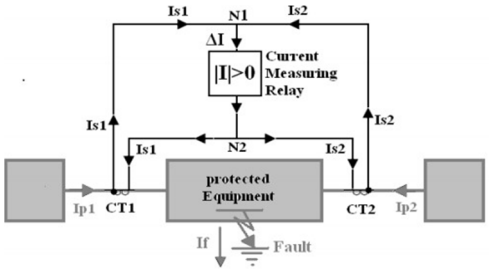

Fig. 1 Current Balance Differential protection

The evolution of relay protection began with high-current relay protection, from which the Discriminatory Short Circuit Protection (DSCP) scheme emerged. DSCP differs from 'overload' protection, incorporating time-based relay operation to safeguard devices thermally. The AOCR Protection system, derived from DSCP, addresses challenges in microgrid operation modes, adapting to distinct short circuit attributes [20].

Microgrids, operating in both grid-connected and island modes, experience varied short circuit conditions, limiting the effectiveness of traditional overcurrent protection. AOCRP accommodates these complexities by enabling adjustments based on grid conditions, facilitated through external communication technology [21]. However, incorporating microgrid configurations into the relay introduces inherent inefficiencies, particularly in intricate network structures, potentially leading to malfunctions during unforeseen events [22].

Adaptive Protection Scheme: Fig. 2 illustrates an adaptive protection scheme with two approaches.

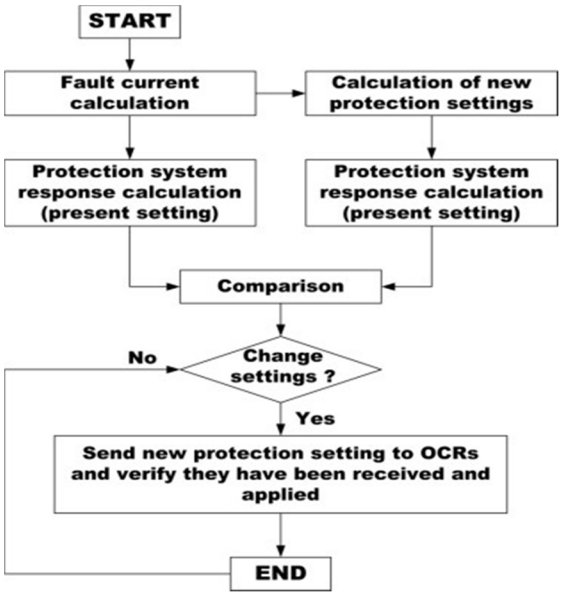

Fig. 2: Adaptive overcurrent protection algorithm

The first approach responds to alterations in the network, adjusting configurations, linking or disconnecting Distributed Generators (DGs), and transitioning between islanded and grid-connected modes. This approach involves real-time calculation and modification of settings, requiring robust decision-making capabilities [20].

IV. PROBLEM STATEMENT AND SYSTEM DESCRIPTION

In response to the identified challenges, there emerges a compelling need for a holistic solution in the form of a combined adaptive overcurrent relay and differential relay protection scheme tailored for smart microgrid systems. This envisioned protection system must possess dynamic adaptability to grid changes, incorporating self-monitoring and self-healing capabilities. Leveraging artificial intelligence (AI) techniques such as neural and fuzzy methods, the microprocessor/numerical relay technology should optimize and adapt seamlessly. The protection strategy must be customized for various zones and equipment within the microgrid, ensuring cost-effectiveness, reliability, and efficiency in both autonomous and grid-connected modes.

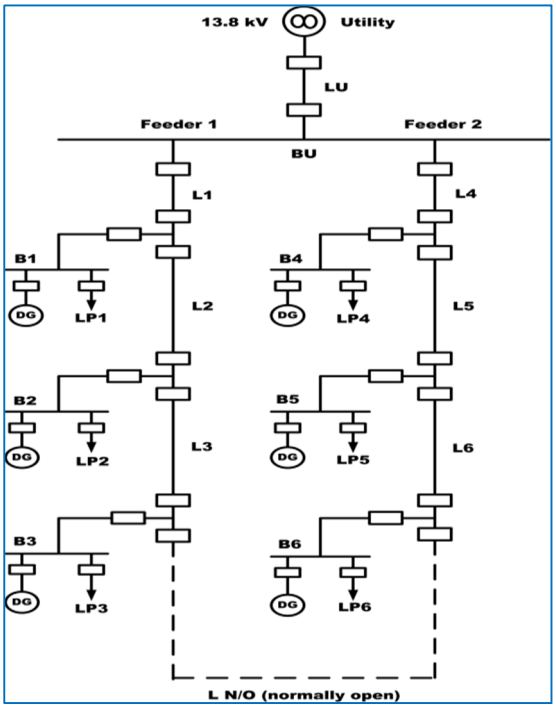

Fig. 3 System under study

This research paper is dedicated to securing the AC microgrid system in both grid-connected and islanded modes, employing a test microgrid system as depicted in Fig 3. Subsequent sections delve into a meticulous examination of the load flow within the AC microgrid system for both operational modes.

1) *System Parameters:*Utility grid-rated capacity = 13.8 kV; DG1 to DG6 rating = 0.2 MW; The power factor for all DGs = 0.9; Load points LP1, LP2, LP4, LP5 rating = 0.2 MW; Load points LP3,; LP6 rating = 0.1 MW; The power factor for all load points (LPs) = 0.9
2) *Protection Settings:* Line and bus differential relay CT ratio = 150/5; Load points CT ratio = 150/5; $I_{DIFFPKP\ MIN}$ = 0.05pu (0.25A); $I_{Breakpoint}$ = 1pu (5A); K_1 = 20%; K_2 = 98%
3) *Grid mode:* Phase pickup = 477 A; Ground pickup = 735 A; Island modes:; Phase pickup = 18 A; Ground pickup = 29 A.

V. FINDINGS AND EXPLORATION

In the AC electrical power distribution network like a power system network or microgrid system operating in both modes of operation in normal operating conditions the 3-phase voltage and current waveforms are sinusoidal in nature with a 50 Hz frequency. But, when 3-phase symmetrical short circuit (SC) faults like LLL, LLLG, or unsymmetrical short circuit (SC) faults like LG, LL, and LLG have occurred in the power system or microgrid system operating in both modes of operation then the magnitude of the SC voltage V_{SC} is decreased to the zero or nearest to the zero value and SC fault current ISC is increased to the very high value in a very short period.

A. Abnormal Operating Condition

Fig. 4 shows the microgrid system model with one DG connection when 3-phase faults occurred on line L1. In this model, the microgrid system is operated in the grid- connected mode of operation with one 0.2 MW DG and one 0.2 MW parallel RLC load point (LP) connected in parallel with the DG at the lower end of the power distribution buses. The 3-phase sinusoidal voltage and current measurement before and after the fault occurrence on line L1 in the microgrid system is done by using the 2 scope blocks connected to the 3-phase V-I measurement bus bar. This microgrid system model is formed in the MATLAB/Simulink software environment.

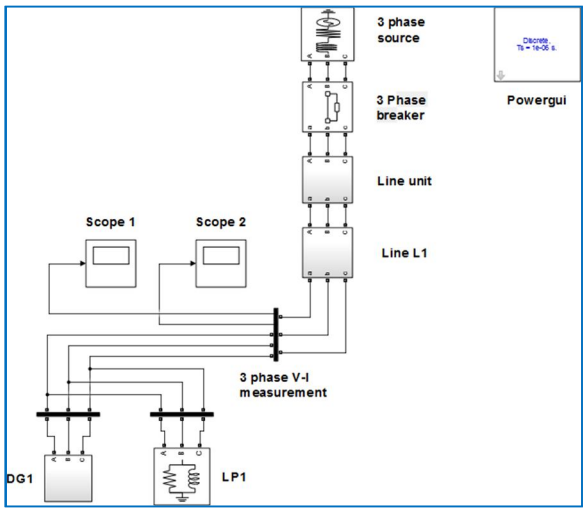

Fig. 4: Microgrid system with one DG connection in faulty condition

This diagram shows the load flow report table for the microgrid system with one DG connection in the faulty condition. In this table, the load flow for one 3-phase source, one 3-phase RLC load, and two buses are shown.

	Block type	Bus type	Bus ID	Vbase (kV)	Vref (pu)	Vangle (deg)	P (MW)	Q (Mv...	Qmin (Mvar)	Qmax (Mvar)	V_LF (pu)	Vangle_LF (deg)	P_LF (MW)	Q_LF (Mvar)	Block Name
1	RLC Load 2		*2*	10.80	1	0.00	0.20	0.10	-Inf	Inf	0.9999	-0.01	0.20	0.10	Three-Phase Parallel RLC Load
2	Bus	-	*3*	100.00	1	0.00	0.00	0.00	0.00	0.00	0.1079	-0.01	0.00	0.00	/Distributed Parameters ...
3	Bus	-	*1*	100.00	1	0.00	0.00	0.00	0.00	0.00	0.1080	0.00	0.00	0.00	/Distributed Parameters ...
4	Vsrc	swing	*5*	10.80	1	0.00	0.01	0.00	-Inf	Inf	1	0.00	0.20	0.08	Three-Phase Source

Fig. 5: Load flow report of the microgrid system with one DG connection in faulty condition

Fig. 6 shows the 3-phase voltage magnitude before and after the fault occurrence on the line L1 with the 50 Hz frequency. In this result, initially, when the microgrid system is operated in the normal operating condition the 3- phase voltage is sinusoidal in nature from 0 to 1 second. The magnitude of this sinusoidal voltage is up to 10 kV from 0 to 1 second in the normal condition. But, when 3 phase SC fault is occurred on the line L1 at 1 second that time 3 phase voltage magnitude suddenly drops to the zero value. This voltage magnitude remains zero till the fault is cleared completely on line L1 in the microgrid system.

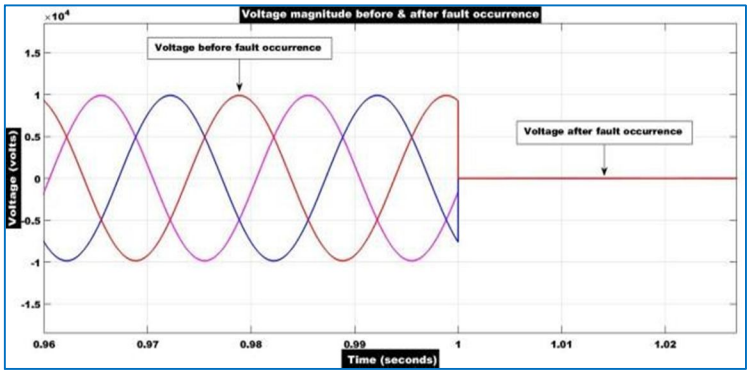

Fig. 6: Voltage magnitude before and after the fault occurrence

Fig. 7 shows the 3-phase sinusoidal current magnitude before and after the fault occurrence on the line L1 with the 50 Hz frequency. In this result, initially, when the microgrid system is operated in the normal operating condition the 3-phase current is sinusoidal in nature with a small current magnitude from 0 to 1 second. But, when 3 phase SC fault occurs on the line L1 at 1 second that time 3 phase current magnitude drastically increases to a very large amount. This current magnitude remains high till the fault is cleared completely on line L1 in the microgrid system.

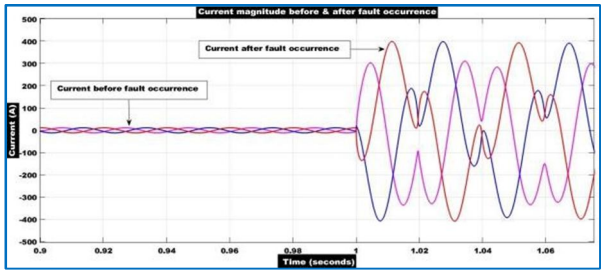

Fig. 7: Current magnitude before and after the fault occurrence

1) Microgrid System with One DG Connection for LLG Fault on Line L1

In this section, the voltage and current magnitude nature concerning the time domain for various symmetrical and unsymmetrical faults that occurred in the AC microgrid system are discussed. The voltage of the phase where the fault occurs instantaneously drops to zero value and current increases to the maximum value after the fault occurrence at that phase. The microgrid system model for any of these symmetrical or unsymmetrical faults is formed in the MATLAB/Simulink software environment, load flow reports are taken from the powergui block and results for each of the faults are shown for validation and discussion purposes. Fig. 8 shows the microgrid system model with one DG connection when an LLG fault has occurred on line L1.

In this model, the microgrid system is operated in the grid- connected mode of operation with one 0.2 MW DG and one 0.2 MW parallel RLC load point (LP) connected in parallel with the DG at the lower end of the power distribution buses. The 3-phase sinusoidal voltage and current measurement before and after the fault occurrence on line L1 in the microgrid system is done by using the 2 scope blocks connected to the 3-phase V-I measurement bus bar. This microgrid system model is formed in the MATLAB/Simulink software environment.

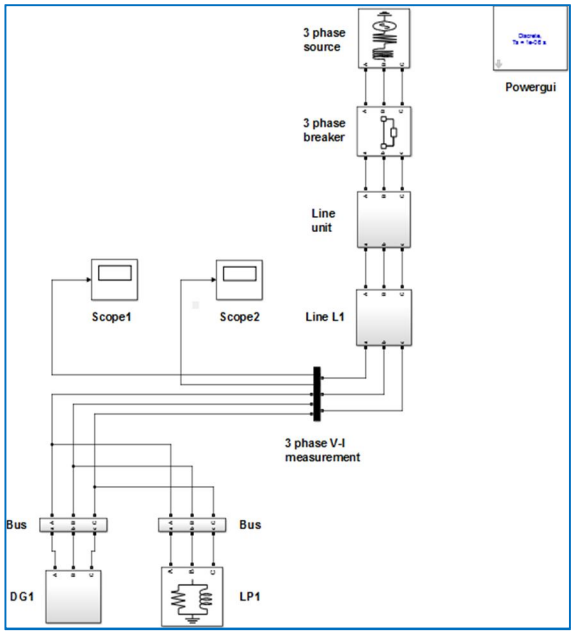

Fig. 8: Microgrid system with one DG connection for LLG fault on line L1

Fig. 9 shows the load flow report table for the microgrid system with one DG connection for the LLG fault that occurred on line L1. In this table, the load flow for one 3- phase source, one 3-phase RLC load, and three buses are shown.

	Block type	Bus type	Bus ID	Vbase (kV)	Vref (pu)	Vangle (deg)	P (MW)	Q (Mv...	Qmin (Mvar)	Qmax (Mvar)	V_LF (pu)	Vangle_LF (deg)	P_LF (MW)	Q_LF (Mvar)	Block Name
1	RLC Load 2	-	*1*	13.80	1	0.00	0.20	0.10	-Inf	Inf	0.922...	21.96	0.00	0.00	Three-Phase Parallel RLC Load
2	Bus	-	*2*	100.00	1	0.00	0.00	0.00	0.00	0.00	0.1380	-0.00	0.00	0.00	...
3	Bus	-	*3*	100.00	1	0.00	0.00	0.00	0.00	0.00	0.1380	-0.00	0.00	0.00	...
4	Bus	-	*4*	100.00	1	0.00	0.00	0.00	0.00	0.00	0.1380	-0.00	0.00	0.00	...
5	Vsrc	swing	*5*	13.80	1	0.00	0.01	0.00	-Inf	Inf	1	0.00	0.00	-0.00	Three-Phase Source

Fig 9: Load flow report of the microgrid system with one DG connection for LLG fault on line L1

Fig 10 shows the 3-phase voltage magnitude for the LLG fault on line L1 before and after the fault occurrence with the 50 Hz frequency. In this result, initially, when the microgrid system is operated in the normal operating condition the 3-phase voltage is sinusoidal in nature from 0 to 1 second.

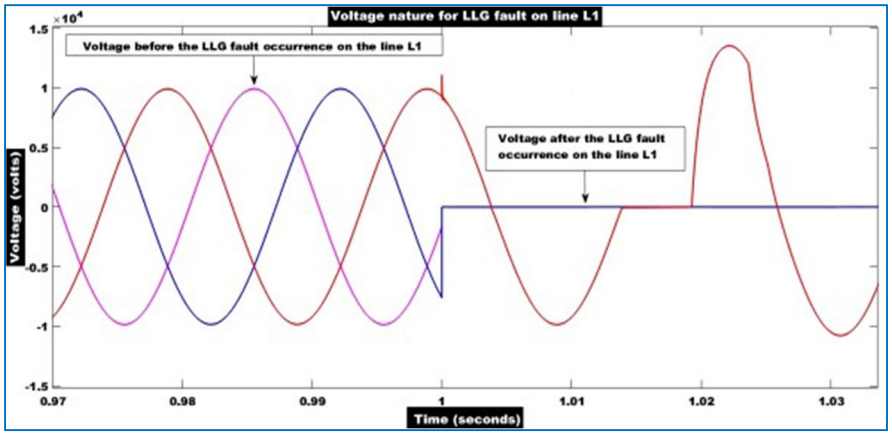

Fig. 10: Voltage nature for LLG fault on line L1 before and after the fault occurrence

The magnitude of this sinusoidal voltage before the fault occurrence is up to 10 kV from 0 to 1 second in normal operating conditions. But, when 3 phase SC LLG fault occurred on line L1 at 1 second that time voltage of the two phases dropped to zero instantaneously and the remaining one-phase voltage increased up to 1.14 kV sinusoidally due to this LLG fault on line L1. The voltage of these two phases remains zero till the LLG fault is cleared completely on line L1 in the microgrid system.
Fig 11 shows the 3-phase sinusoidal current magnitude for LLG fault on line L1 before and after the fault occurrence with the 50 Hz frequency.

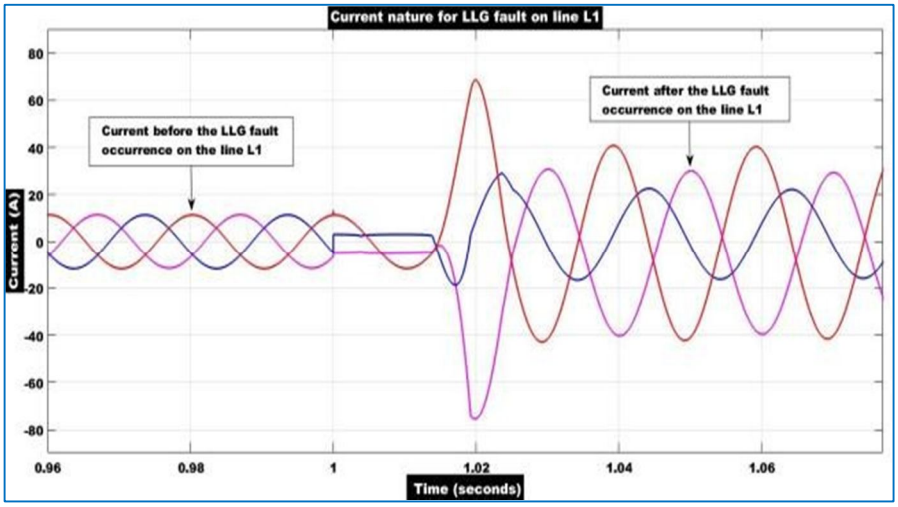

Fig. 11: Current nature for LLG fault on line L1 before and after the fault

In this result, initially, when the microgrid system is operated in the normal operating condition the 3-phase current is sinusoidal in nature with 10 to 15 A current magnitudes from 0 to 1 second. But, when 3 phase SC LLG fault occurs on line L1 at 1 second that time two phases' current magnitude increases up to 70 A in a very small-time duration and the current of the remaining phase also increases up the 30 A in a small-time duration due to the LLG fault on the line L1. This current magnitude remains high till the LLG fault is cleared completely on line L1 in the microgrid system.

2) Microgrid System with One DG Connection for LLLG Fault on Line L1

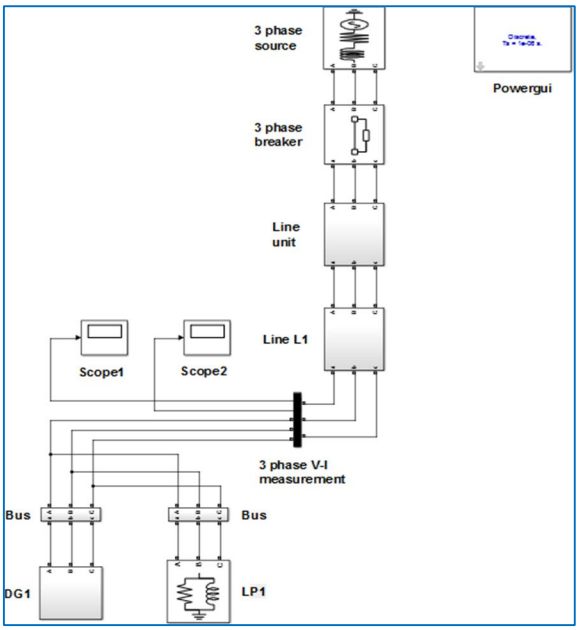

Fig 12: Microgrid system with one DG connection for LLLG fault on line L1

Fig 12 shows the microgrid system model with one DG connection when an LLLG fault has occurred on line L1. In this model, the microgrid system is operated in the grid- connected mode of operation with one 0.2 MW DG and one 0.2 MW parallel RLC load point (LP) connected in parallel with the DG at the lower end of the power distribution buses. The 3-phase sinusoidal voltage and current measurement before and after the LLLG fault occurrence on line L1 in the microgrid system is done by using the 2 scope blocks connected to the 3-phase V-I measurement bus bar. This microgrid system model is formed in the MATLAB/Simulink software environment.

Fig. 13 shows the load flow report table for the microgrid system with one DG connection for the LLLG fault that occurred on line L1. In this table, the load flow for one 3- phase source, one 3-phase RLC load, and three buses are shown.

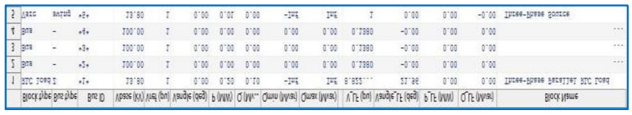

Fig. 13: Load flow report of the microgrid system with one DG connection for LLLG fault on line L1

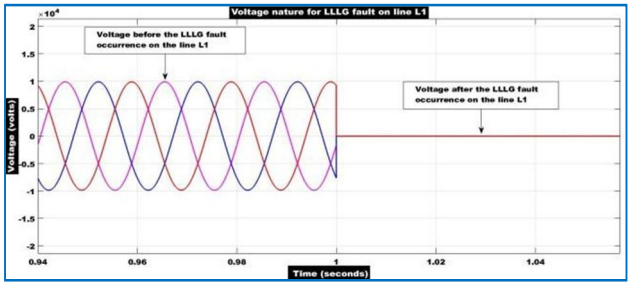

Fig. 14: Voltage nature for LLLG fault on line L1 before and after the fault

Fig. 14 illustrates the magnitude of the three-phase voltage for an LLLG fault on line L1, both before and after the fault, at a frequency of 50 Hz. During the usual working conditions of the microgrid system, the 3-phase voltage exhibits a sinusoidal waveform ranging from 0 to 1 second. The amplitude of this sinusoidal voltage before the fault event is 10 kV, ranging from 0 to 1 second, under normal operating conditions. However, when a three-phase short circuit line-to-line-to-ground fault occurs on line L1 at 1 second, the voltage of all three phases instantaneously drops to zero as a result of this LLLG failure on line L1. The voltage of these three phases remains at zero until the LLLG fault is completely resolved on line L1 in the microgrid system.

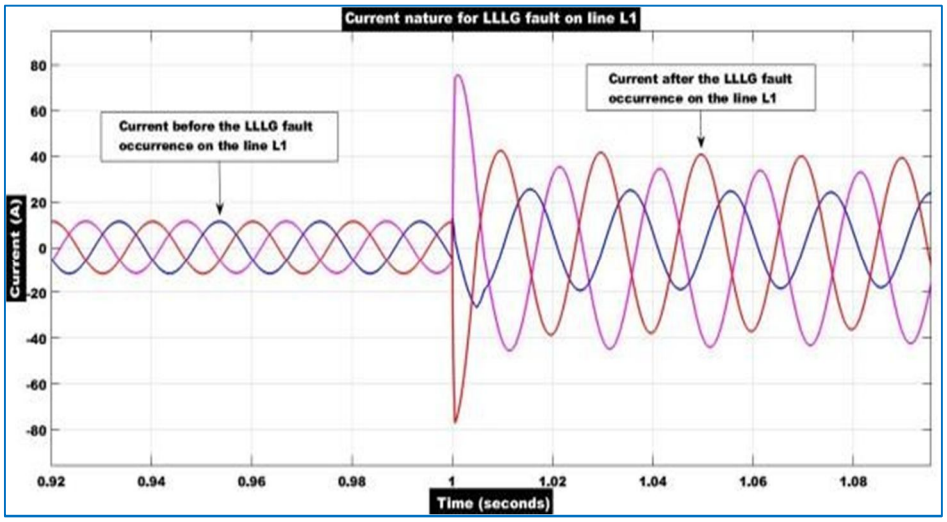

Fig 15: Current of LLLG fault on line L1 before and after the fault

Fig.15 illustrates the magnitude of the sinusoidal current in three phases for an LLLG fault on line L1, both before and after the fault has occurred, with a frequency of 50 Hz. During typical operation of the microgrid system, the 3- phase current exhibits a sinusoidal waveform with current magnitudes ranging from 10 to 15 A, during the time interval of 0 to 1 second. However, when a three-phase short circuit to line-to-line-to-ground fault occurs on line L1 at 1 second, the magnitudes of the currents in two phases increase instantaneously to 78 A, while the current in the remaining phase also increases instantaneously to 24 A due to the LLLG fault on line L1. The magnitude of the current will stay elevated until the LLLG fault on line L1 in the microgrid system is completely resolved.

B. Protection of AC Microgrid System from LLL-G Faults

In this section, examine the safeguarding of AC microgrid systems against three-phase SC LLLG failures in both grid-connected and islanded modes of operation. To study, analyze, and discuss the results, we examined this microgrid system in two specific case studies, referred to as Case Study - 1 and Case Study - 2. The load flow report of the microgrid system is obtained independently for each case study in both modes of operation using the power GUI block. The time-domain simulations, including outcomes, are comprehensively presented and analyzed for each case study, encompassing both modes of operation. The intricate models of microgrid systems being examined in both operational modes are created using the MATLAB/Simulink software environment.

Case Study - 1: Protecting an AC microgrid system using a current differential relay protection scheme in the event of a three-phase single LLG fault occurring on line L1 in both modes of operation (protecting faults occurring within the protected zone of the microgrid structure, such as faults on feeders, lines, buses, etc.).

Case Study - 2 Protecting an AC microgrid system by implementing an adaptive overcurrent relay protection scheme. This scheme is designed to respond to a 3-phase SC LLLG fault occurring at the 3-phase parallel RLC load point LP1, in both modes of operation. It ensures the protection of the microgrid system even when 3-phase faults occur outside the zone of protection, such as faults at DGs (distributed generators), loads, etc.

1) Case Study 1: Current Differential Relays

a) Islanded Mode of Operation

As seen in Fig.16, a comprehensive model of the microgrid network operating in island mode is displayed. Here, in the MATLAB/Simulink environment, the 3-phase LLLG fault is generated on the 3-phase line L1.

The table in Fig.17 displays the load flow evaluation for the microgrid network in the islanded mode of functioning. This table provides the load flow estimate for each bus. The block name, block type, bus type, and bus ID of every part are specified here.

This table displays the base voltage of the 3-phase RLC source, as well as the base voltage at each bus and the base voltage at the 3-phase parallel RLC load terminals. It displays the reference voltage of each bus in per unit (pu) value. The calculation of active power is expressed in megawatts (MW), whereas the calculation of reactive power is expressed in Megavars (Mvar). The voltage load flow is in pu, and the voltage load flow angle is measured in degrees. All load flow estimates for the islanded mode functionality are derived and obtained from the power Gui block of the microgrid system's architecture when it is run in islanded mode.

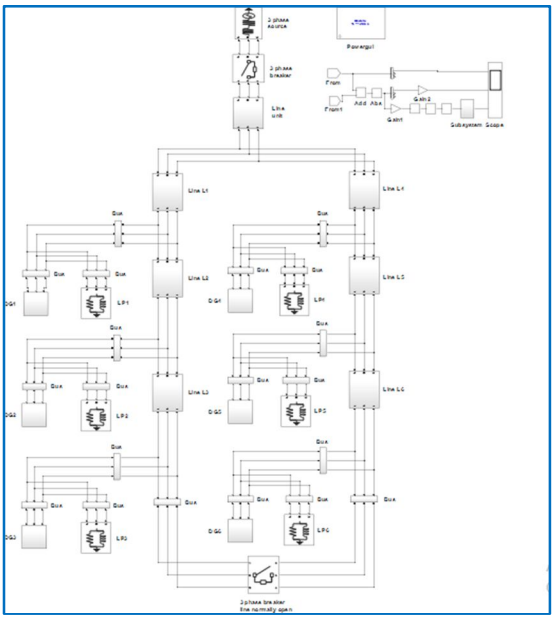

Fig. 16: Microgrid islanded mode of operation

Fig. 17: Load flow for an islanded mode of operation

b) Results for Islanded Mode of Operation

Fig. 18 displays the outcomes of the microgrid system when functioning in islanded mode. A 3-phase LLLG defect is intentionally induced on the L1 phase of a 3-phase line, resulting in the display of 3 outcomes. The purpose of this is to safeguard both the consumers and equipment of the microgrid system from any 3 phase faults that may occur within the protected region. The existing differential relay protection technique effectively resolves these errors within a time frame of 0.1 to 0.2 seconds.

- *Radial Breaker Unit 1 (RBU1) Current*

During the disconnection of the microgrid system from the utility grid, the RBU1 current undergoes oscillations with a duration ranging from 0 to 0.1 seconds. During islanded mode, if line L1 fails, the current in RBU1 increases to 38 A for a single cycle. Following the resolution of the fault at 0.12 seconds on line L1, the current in RBU1 became stable and continued to flow steadily from 0.12 to 0.2 seconds.

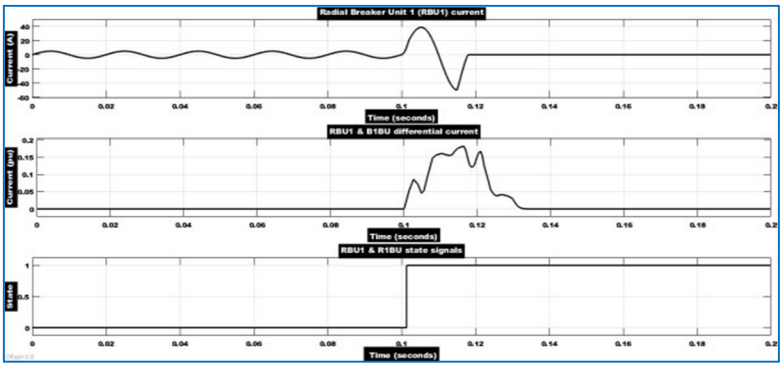

Fig. 18: Islanded mode of operation

- *Differential Current-RBU1 and B1BU, the Radial Breaker Units*

In islanded mode, the differential current waveforms remain identical to those in grid-connected mode. The differential current waveform exhibits a rapid decrease in the current signal, and the relay encountered a peak current of 0.18 per unit (pu) between 0.1 and 0.13 seconds in islanded mode.The differential relay successfully detected and resolved the line L1 fault in islanded mode within 0.1 and 0.14 seconds. Between 0.14 and 0.2 seconds, the differential current remains at zero until the finish.

- *State signals of the Radial breaker unit 1 (RBU1) and the radial 1 breaker unit (R1BU).*

This outcome demonstrates that the RBU1 and R1BU status signals in the islanded mode closely resemble those in the grid-connected mode.

2) Case Study 2: Adaptive Overcurrent Relays

a) Grid-connected mode.

Fig. 19 depicts the intricate model of the microgrid network operating in the grid-connected mode. The 3-phase LLLG fault is induced on the 3-phase parallel RLC load point LP1 within the MATLAB/Sim software environment.

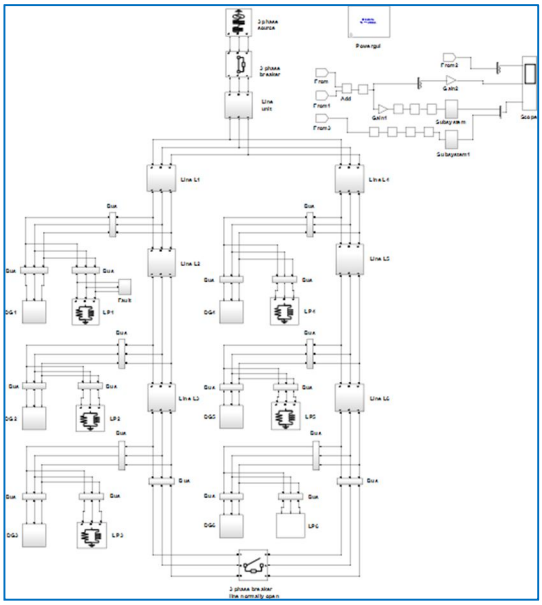

Fig. 19 Microgrid network operating in grid-connected mode.

Fig. 20 displays the table that represents the load flow evaluation of a microgrid system in the grid-connected state of performance. This table provides the load flow estimations for each bus. Here, the block name, block type, bus type, and bus ID of each component are specified. The table displays the base voltage of the 3-phase RLC source, as well as the base voltage at each bus and the base voltage at the 3-phase parallel RLC load terminals. It displays the reference voltage of each bus in per unit (pu) measurement. Calculate the active power in megawatts (MW), reactive power in mega vars (Mvar), voltage load flow per unit (pu), and voltage load flow angle in degrees. All load flow calculations for the grid-connected mode of operation are derived and extracted from the power Gui block of the microgrid framework's model during its operation in the grid-connected state.

	Block type	Bus type	Bus ID	Vbase (kV)	Vref (pu)	Vangle (deg)	P (MW)	Q (Mv...	Qmin (Mvar)	Qmax (Mvar)	V_LF (pu)	Vangle_LF (deg)	P_LF (MW)	Q_LF (Mvar)	Block Name
1	RLC load 2		*1*	13.80	1	0.00	0.20	0.10	-Inf	Inf	3.926...	-119.91	0.00	0.00	Three-Phase Parallel RLC Load2
2	RLC load 2		*2*	13.80	1	0.00	0.20	0.10	-Inf	Inf	7.036...	106.10	0.00	0.00	Three-Phase Parallel RLC Load4
3	RLC load 2		*3*	13.80	1	0.00	0.20	0.10	-Inf	Inf	7.036...	106.10	0.00	0.00	Three-Phase Parallel RLC Load5
4	RLC load 2		*4*	13.80	1	0.00	0.20	0.10	-Inf	Inf	4.476...	171.91	0.00	0.00	Three-Phase Parallel RLC Load1
5	RLC load 2		*5*	13.80	1	0.00	0.20	0.10	-Inf	Inf	3.922...	-119.30	0.00	0.00	Three-Phase Parallel RLC Load
6	Bus	-	*6*	100.00	1	0.00	0.00	0.00	0.00	0.00	0.0040	-136.46	0.00	0.00	L1/Distributed Parameters Line
7	Bus	-	*7*	100.00	1	0.00	0.00	0.00	0.00	0.00	0.0040	-136.46	0.00	0.00	L1/Distributed Parameters Line
8	Bus	-	*8*	100.00	1	0.00	0.00	0.00	0.00	0.00	4.600...	156.04	0.00	0.00	L2/Distributed Parameters Line
9	Bus	-	*9*	100.00	1	0.00	0.00	0.00	0.00	0.00	4.600...	156.04	0.00	0.00	L2/Distributed Parameters Line
10	Bus	-	*10*	100.00	1	0.00	0.00	0.00	0.00	0.00	5.456...	84.13	0.00	0.00	L3/Distributed Parameters Line
11	Bus	-	*11*	100.00	1	0.00	0.00	0.00	0.00	0.00	5.456...	84.13	0.00	0.00	L3/Distributed Parameters Line
12	Bus	-	*12*	100.00	1	0.00	0.00	0.00	0.00	0.00	5.456...	84.13	0.00	0.00	L6/Distributed Parameters Line
13	Bus	-	*13*	100.00	1	0.00	0.00	0.00	0.00	0.00	5.456...	84.13	0.00	0.00	L6/Distributed Parameters Line
14	RLC load 2		*14*	13.80	1	0.00	0.20	0.10	-Inf	Inf	4.476...	171.91	0.00	0.00	Three-Phase Parallel RLC Load3
15	Bus	-	*15*	100.00	1	0.00	0.00	0.00	0.00	0.00	4.600...	156.04	0.00	0.00	L5/Distributed Parameters Line
16	Bus	-	*16*	100.00	1	0.00	0.00	0.00	0.00	0.00	4.600...	156.04	0.00	0.00	L5/Distributed Parameters Line
17	Bus	-	*17*	100.00	1	0.00	0.00	0.00	0.00	0.00	0.0040	-136.46	0.00	0.00	L4/Distributed Parameters Line
18	Bus	-	*18*	100.00	1	0.00	0.00	0.00	0.00	0.00	0.0040	-136.46	0.00	0.00	L4/Distributed Parameters Line
19	Bus	-	*19*	100.00	1	0.00	0.00	0.00	0.00	0.00	0.0390	-62.23	0.00	0.00	L7/Distributed Parameters Line
20	Bus	-	*20*	100.00	1	0.00	0.00	0.00	0.00	0.00	0.0390	-62.23	0.00	0.00	L7/Distributed Parameters Line
21	Vacc	swing	*21*	13.80	1	0.00	0.01	0.00	-Inf	Inf	1	0.00	0.00	-0.00	Three-Phase Source

Fig. 20: Load flow for grid-connected mode

b) Results during Grid-Connected Mode of Operation

In the context of the microgrid system's grid-connected mode of operation, as depicted in Fig. 21, a comprehensive analysis of a 3-phase LLLG fault occurring at load point LP1 at 0.1 seconds reveals three key outcomes. This examination serves as a crucial aspect of safeguarding the microgrid system's consumers and equipment, offering protection against 3-phase faults that may arise beyond the designated protection zone (e.g., faults occurring at DGs, loads, etc.). The adaptive overcurrent relay protection scheme efficiently clears these faults within the timeframe of 0.1 to 0.2 seconds.

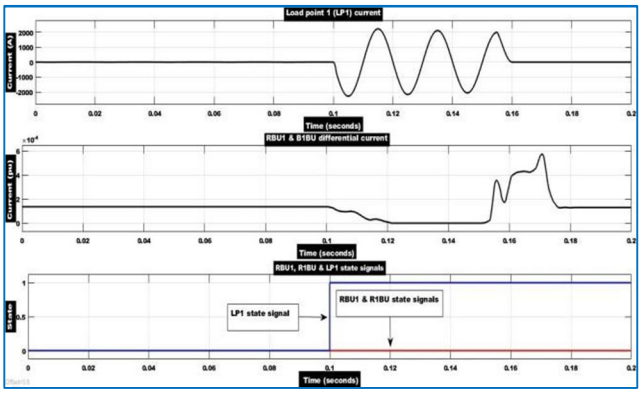

Fig. 21: Grid-connected mode of operation

- *Load Point 1 (LP1) Current*

The LP1 current initially flows consistently from zero up to 0.1 seconds. However, when a fault occurs at load LP1 at 0.1 seconds, the relay registers a substantial current spike, reaching up to 2220 A between 0.1 and 0.16 seconds. The adaptive overcurrent relay promptly operates and trips the respective circuit breaker after 0.1 seconds, successfully clearing the fault beyond the protection zone by 0.16 seconds. Subsequently, the LP1 current continues to flow consistently from 0.16 to 0.2 seconds, with the differential relay remaining inactive for faults occurring outside the zone of protection.

- *Radial Breaker Unit 1 (RBU1) and Bus 1 Breaker Unit (B1BU) Differential Current*

Before the fault, the current flowing from circuit breaker units RBU1 and B1BU of line L1 is approximately 0.00015 pu. When the fault occurs at load LP1, the maximum differential current from line L1 reaches up to 0.00058 pu with some disturbances in the waveform. Post fault clearance, the differential current returns to its initial value of 0.00015 pu.

- *Radial Breaker Unit 1 (RBU1), Radial 1 Breaker Unit (R1BU), and Load Point 1 (LP1) State Signals*

This result displays the state signals of two circuit breakers, RBU1 and R1BU, along with the LP1 state signal. Both circuit breakers' state signals (RBU1 and R1BU) remain constant at zero from 0 to 0.2 seconds. Simultaneously, the LP1 state signal flows consistently from 0 to 0.1 seconds. At 0.1 seconds, the LP1 state signal transitions to state 1, maintaining a stable flow from 0.1 to 0.2 seconds.

VI. CONCLUSION

This paper concludes that this protection scheme for the microgrid system under the study operated effectively and protected the overall microgrid system from 3 phases of SC symmetrical LLLG faults are occurred in both grid- connected and islanded modes of operation. The current differential relay protection scheme operated successfully and protects the consumers as well as equipment connected in the microgrid system when 3-phase SC faults occur inside the zone of protection. Also, the adaptive overcurrent relays protection scheme operated successfully and protected the consumers as well as equipment connected in the microgrid system when 3-phase SC faults occurred outside the zone of protection (e.g., when faults occurred at DGs, loads, etc.).

Also, this microgrid protection scheme shows feasibility and effectiveness in both modes of operation under the changing SC fault current level and varying fault impedance in the microgrid system. This protection scheme can be effectively implemented for symmetrical faults like LLL, and LLLG faults. This protection scheme improves the reliability, power quality, efficiency, and safety operation of both consumers as well as equipment connected to the microgrid system by clearing the 3-phase SC faults in the minimum possible time and by protecting the overall microgrid system effectively.

BIBLIOGRAPHY

[1] H. Laaksonen and S. Repo, "Adaptive protection scheme for microgrids with distributed energy resources," IEEE Transactions on Power Delivery, vol. 35, no. 2, pp. 967–977, Apr. 2020.
[2] M. E. Elkhatib and M. S. El-Moursi, "Differential protection of microgrid feeders with high penetration of distributed energy resources," Electric Power Systems Research, vol. 189, pp. 106676, Dec. 2021.
[3] S. Mirsaeidi, D. Said, and A. Mustafa, "A comprehensive review of microgrid protection challenges and solutions," Renewable and Sustainable Energy Reviews, vol. 112, pp. 410–424, Sept. 2019.
[4] J. C. Vasquez and J. M. Guerrero, "Protection strategies for inverter-dominated microgrids," IEEE Access, vol. 10, pp. 45812–45825, 2022.
[5] A. G. Phadke and J. S. Thorp, "Role of differential protection in modern distribution networks," IEEE Power & Energy Magazine, vol. 18, no. 3, pp. 62–71, May–Jun. 2020.
[6] K. Saleh and O. A. Mohammed, "Adaptive overcurrent protection for microgrids considering DER variability," International Journal of Electrical Power & Energy Systems, vol. 129, pp. 106778, July 2021.
[7] P. Mahat and Z. Chen, "Protection coordination of microgrids using hybrid relay schemes," IET Generation, Transmission & Distribution, vol. 17, no. 8, pp. 1652–1662, 2023.
[8] Y. Li and M. Shahidehpour, "Microgrid protection and control: State-of-the-art review," IEEE Transactions on Smart Grid, vol. 13, no. 5, pp. 4321–4334, Sept. 2022.
[9] R. Majumder and B. Chaudhuri, "Protection of active distribution networks with microgrids," Electric Power Components and Systems, vol. 48, no. 6, pp. 521–533, 2020.
[10] T. S. Sidhu and M. S. Sachdev, "Advances in microgrid protection using intelligent relays," IEEE Transactions on Power Systems, vol. 39, no. 1, pp. 115–126, Jan. 2024.

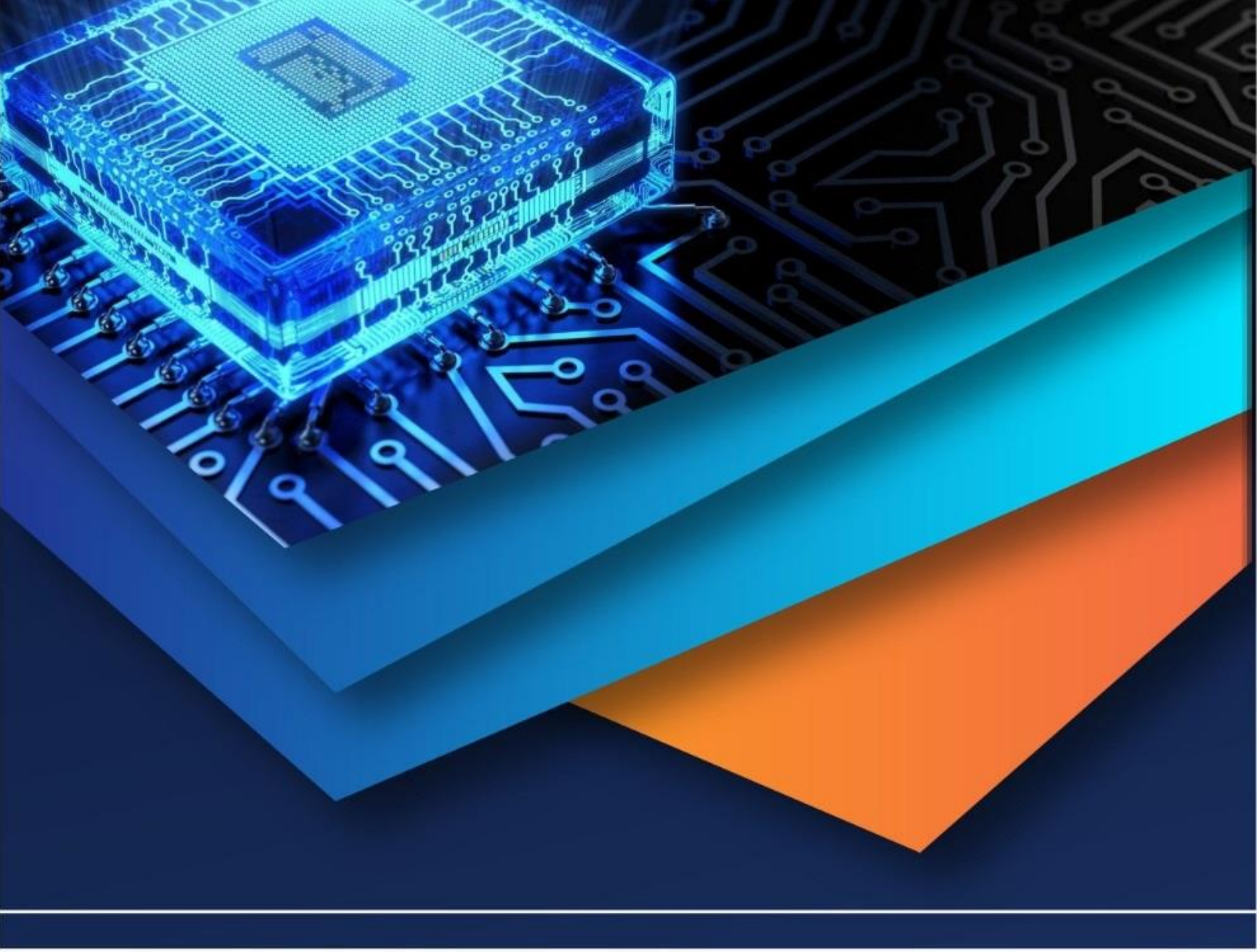

10.22214/IJRASET

45.98

IMPACT FACTOR: 7.129

IMPACT FACTOR: 7.429

INTERNATIONAL JOURNAL FOR RESEARCH

IN APPLIED SCIENCE & ENGINEERING TECHNOLOGY